J. Cent. South Univ. (2015) 22: 2339−2347
DOI: 10.1007/s11771-015-2759-4

Springer

Upper bound analytical solution for surrounding rock pressure of shallow unsymmetrical loading tunnels

LEI Ming-feng(雷明锋)[1, 2], PENG Li-min(彭立敏)[1], SHI Cheng-hua(施成华)[1],
XIE You-jun(谢友均)[1], TAN Li-xin(谭立新)[2]

1. School of Civil Engineering, Central South University, Changsha 410075, China;
2. China Construction Fifth Engineering Division Corp., Ltd., Changsha 410004, China

Abstract: By combining the results of laboratory model tests with relevant flow rules, the failure mode of shallow unsymmetrical loading tunnels and the corresponding velocity field were established. According to the principle of virtual power, the upper bound solution for surrounding rock pressure of shallow unsymmetrical loading tunnel was derived and verified by an example. The results indicate that the calculated results of the derived upper bound method for surrounding rock pressure of shallow unsymmetrical loading tunnels are relatively close to those of the existing "code method" and test results, which means that the proposed method is feasible. The current code method underestimates the unsymmetrical loading feature of surrounding rock pressure of shallow unsymmetrical loading tunnels, so it is unsafe; when the burial depth is less or greater than two times of the tunnel span and the unsymmetrical loading angle is less than 45°, the upper bound method or the average value of the results calculated by the upper bound method and code method respectively, is comparatively reasonable. When the burial depth is greater than two times of the tunnel span and the unsymmetrical loading angle is greater than 45°, the code method is more suitable.

Key words: tunnel; shallow buried tunnel; unsymmetrical loading; ultimate analysis method; upper bound solution

1 Introduction

Restricted by geological conditions and line direction, the tunnels with entrance and the sections next to mountains and valleys are commonly unsymmetrical loading tunnels. Compared to normal tunnels, the unsymmetrical loading tunnels have complex structural stress and large construction difficulty. Therefore, the engineering accidents and potential risks such as mountain slumping, initial support instability and secondary lining cracking may occur. The basic reason is insufficient knowledge of the characteristics of structural stress and surrounding rock pressure of unsymmetrical loading tunnels, which causes the design scheme to lack pertinence and results in unreasonable construction method and auxiliary measures [1]. Therefore, during the design process, it is crucial to accurately determine the structural stress of unsymmetrical loading tunnels, i.e. surrounding rock pressure [2−3].

At present, the calculation of the surrounding rock pressure of unsymmetrical loading tunnels is mainly the method recommended in the design codes of railway and road tunnels in China. An assumption that the distribution pattern of surrounding rock pressure of unsymmetrical loading tunnels is consistent with the ground slope is made, and then the limit equilibrium analysis method is used to obtain the results [4−5]. For years, it has been applied in engineering practice widely. However, due to too many assumptions, the model is simplified, and the calculated result shows a great difference with the actual situations. The model test results in Ref. [1] show that the method used for calculating the surrounding rock pressure of unsymmetrical loading tunnels, recommended by the above two codes, underestimates the unsymmetrical loading feature, and is likely to bring about safety risks. Therefore, the research on the calculation methods for surrounding rock pressure of unsymmetrical loading tunnels is far from sufficient.

The limit analysis method is popular among the researchers due to its distinct concept and mature theory. The upper and lower bound theorems have been applied to the stability issues of shallow tunnels and useful conclusions are obtained [6−8]. Moreover, based on previous achievements, a certain failure mode is assumed,

Foundation item: Project(2014M560652) supported by China Postdoctoral Science Foundation; Projects(2011CB013802, 2013CB036004) supported by the National Basic Research Program of China
Received date: 2014−05−08; **Accepted date:** 2014−10−20
Corresponding author: SHI Cheng-hua, Professor, PhD; Tel: +86−13787232438; E-mail: 124520238@qq.com

and the corresponding velocity field to obtain the upper-bound solution for the surrounding rock pressure of shallow buried tunnels is built [9−14]. However, these researches do not consider the unsymmetrical loading of terrain, so they can't be applied in shallow-buried unsymmetrical loading tunnels [15].

In this work, the results of model test [1] are taken as the basis to establish the failure mode of surrounding rocks of shallow buried unsymmetrical loading tunnels, and then to derive the upper-bound solution for surrounding rock pressure of shallow-buried unsymmetrical loading tunnels based on the theory of upper bound method. Finally, a comparative analysis is made using application examples.

2 Establishment of failure mode

2.1 Basic assumptions

In order to facilitate the analysis, the following assumptions are made:

1) A tunnel surrounding rock is considered as an ideal elastic plastic body and the material $c-\phi$ relation conforms to Mohr-Coulomb yield criterion.

2) The tunnel section is simplified into the one with vertical wall height H, span $2b$, upper arc rise f, and burial depth h_1 at the midline of tunnel roof. Vertical loads acting on the tunnel vault are q_1 and q_2, respectively, in a linear distribution. The evenly distributed horizontal surrounding rock pressures acting on the side wall are e_1 and e_2, respectively, and $e_i=kq_i$ (i=1, 2), where k is an undetermined parameter, as shown in Fig. 1.

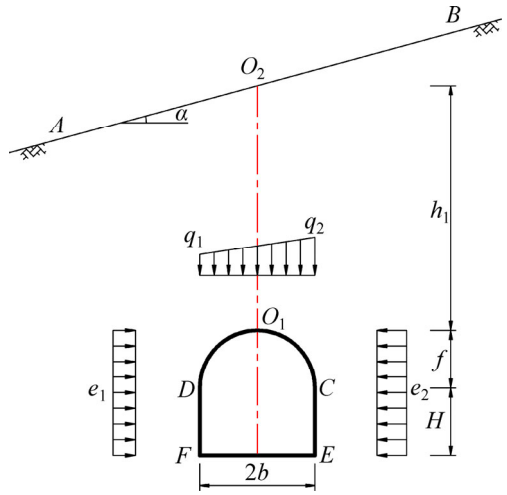

Fig. 1 Distribution mode of surrounding rock pressure

3) The movements of side wall and vault do not impact each other. The internal energy dissipation produced by friction is negligible, and the influence of construction method is not considered.

4) The surrounding rocks in certain ranges above the tunnel vault and below ground surface are restrained by surrounding rock-soil mass, and their displacement is mainly vertical.

2.2 Failure mode

According to the above assumptions and the results of model test [1], it can be derived that the fracture lines on both sides of the tunnel are continuous parabola-like curves and tangent to the basement. Hence, the failure mode of the surrounding rock of shallow-buried unsymmetrical loading tunnel is established, as shown in Fig. 2. As shown, α is the angle of terrain unsymmetrical loading; $\overset{\frown}{AF}$ and $\overset{\frown}{BE}$ are fracture curves in shallow buried and deep-buried sides, respectively; AB is the ground surface line, and $AA_1O_1B_1B$ is the rigid body with only a trend of vertical sliding.

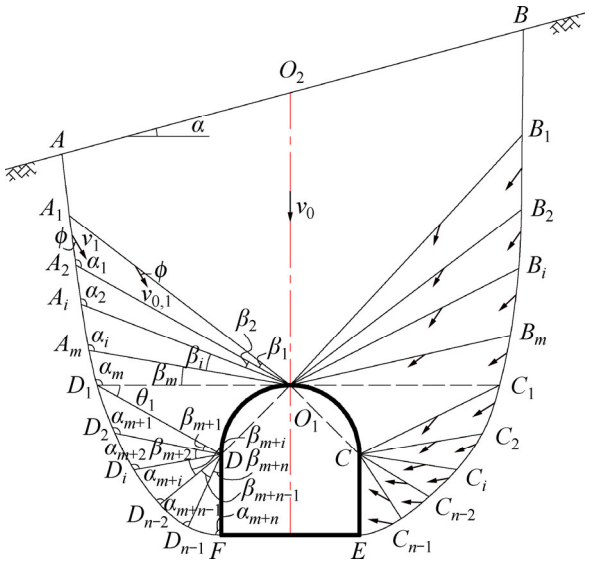

Fig. 2 Failure mode of shallow buried tunnel

The horizontal line passing through vault O_1 discretizes the fracture lines AF and BE into two parts containing m and n sections. With vertexes C and D of side wall and vault O_1 as vertexes, the whole fracture body is divided into several small triangular sliding blocks, of which there are (m−1) blocks in the area above the side wall, and (n−1) blocks in the area below side wall. It is supposed that the included angles between each broken line and fracture line and between two adjacent broken lines are α_i and β_i (i=1, ⋯, m+n), respectively, so the shape of the fracture body composed of all the triangular sliding blocks can be described by $\{\alpha_i, \beta_i\}$. The required target value, i.e. surrounding rock pressure q is the function of $\{\alpha_i, \beta_i\}$, that is, $q=f(\alpha_i, \beta_i)$.

3 Velocity field and vector relation

3.1 Establishment of velocity field

According to assumption 4), the rigid sliding block

above the tunnel vault lies at a certain depth in soil, and is restrained in horizontal direction. So, its velocity vector in horizontal direction is negligible, and the velocity vector is vertical and points downwards.

The rigid sliding blocks $AA_1O_1O_2$ and $A_1A_2O_1$ on the left side of the tunnel are analyzed, as shown in Fig. 3. Suppose that the downward velocity vector of $AA_1O_1O_2$ is v_0, and the calculated friction angle of fracture plane of surrounding rock is ϕ. The relation between velocity vectors, as shown in Fig. 4, can be obtained based on the associated flow rule.

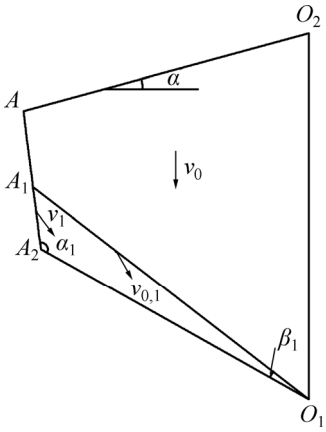

Fig. 3 Velocity vector of sliding block

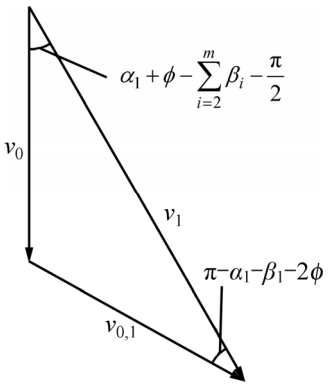

Fig. 4 Vector relationship of v_0−v_1

3.2 Derivation of velocity vector relation

From the vector relation shown in Fig. 4 and sine theorem, it can be seen that the velocity vectors of all broken lines of the quadrilateral sliding block $AA_1O_1O_2$ should satisfy the following recursion relation:

$$\begin{cases} v_1=\dfrac{\cos\left(\phi+\sum_{i=1}^{m}\beta_i\right)}{\sin(\alpha_1+\beta_1+2\phi)}v_0 \\ v_{0,1}=\dfrac{-\cos\left(\sum_{i=2}^{m}\beta_i-\alpha_1-\phi\right)}{\sin(\alpha_1+\beta_1+2\phi)}v_0 \end{cases} \tag{1}$$

Similarly, the velocity vector relations of all broken lines of the triangular sliding block D_1D_2D can be derived as

$$\begin{cases} v_{m+1}=\dfrac{\sin(\alpha_m+2\phi+\theta_1)}{\sin(\alpha_{m+1}+\beta_{m+1}+2\phi)}v_m \\ v_{m,m+1}=\dfrac{\sin(\alpha_{m+1}-\alpha_m+\beta_{m+1}-\theta_1)}{\sin(\alpha_{m+1}+\beta_{m+1}+2\phi)}v_m \end{cases} \tag{2}$$

Further, by reference to the velocity field shown in Fig. 5, for any sliding block $A_iA_{i+1}O_1$ ($D_iD_{i+1}D$) (Fig. 6), the recursion relation of the velocity vectors of all broken lines is

$$\begin{cases} v_{i+1}=\dfrac{\sin(\alpha_i+2\phi)}{\sin(\alpha_{i+1}+\beta_{i+1}+2\phi)}v_i \\ v_{i,i+1}=\dfrac{\sin(\alpha_{i+1}-\alpha_i+\beta_{i+1})}{\sin(\alpha_{i+1}+\beta_{i+1}+2\phi)}v_i \end{cases} \tag{3}$$

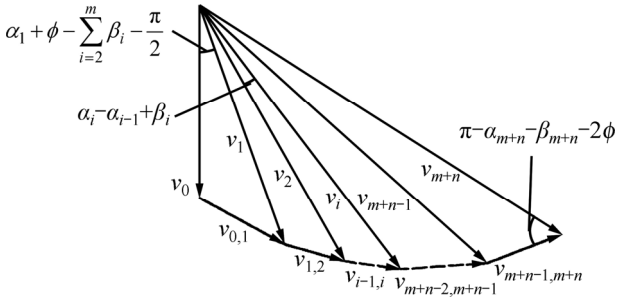

Fig. 5 Velocity field corresponding to failure mode

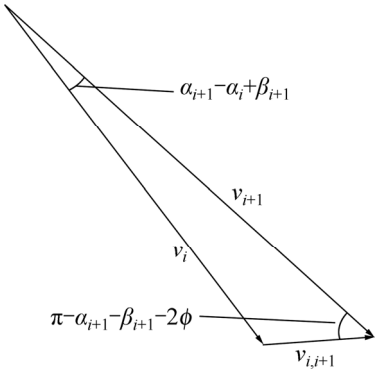

Fig. 6 Velocity vector relationship of block $A_iA_{i+1}O_1$ ($D_iD_{i+1}D$)

In the fracture area above the vault, i=1,⋯, m−1; in the fracture area below the vault, i=m+1,⋯, m+n−1; θ_1 is the angle of $\angle O_1D_1D$; $v_{0,1}$ is the velocity vector of the broken line A_1O_1, v_i (i=1, ⋯, m+n) is the velocity vector of the small section of fracture line, and $v_{i,i+1}$ (i=0,⋯, m+n−1) is the velocity vector of the broken line.

4 Derivation of geometric relations of fracture sliding blocks

4.1 Lengths of broken lines and fracture lines

For sliding block $DD_{n-1}F$, as shown in Fig. 7, the relation between the lengths of broken lines or fracture lines of all velocities can be derived from the geometric relation of the triangle:

$$\begin{cases}\overline{DD_{n-1}}=\dfrac{\sin\alpha_{m+n}}{\sin(\alpha_{m+n}+\beta_{m+n})}\overline{DF}\\ \overline{D_{n-1}F}=\dfrac{\sin\beta_{m+n}}{\sin(\alpha_{m+n}+\beta_{m+n})}\overline{DF}\end{cases}\tag{4}$$

where $\overline{DF}$, $\overline{DD}_{n-1}$ and $\overline{D_{n-1}F}$ are the lengths of the sides of sliding block $DD_{n-1}F$.

Thus, for any sliding block DD_iD_{i+1}, as shown in Fig. 8, there is

$$\begin{cases}\overline{DD_i}=\dfrac{\sin\alpha_{m+i}}{\sin(\alpha_{m+i}+\beta_{m+i})}\overline{DD_{i+1}}\\ \overline{D_iD_{i+1}}=\dfrac{\sin\beta_{m+i}}{\sin(\alpha_{m+i}+\beta_{m+i})}\overline{DD_{i+1}}\end{cases}\quad(i=1,\cdots,n-1)\tag{5}$$

where $\overline{DD_i}$ and $\overline{D_iD_{i+1}}$ are the lengths of the sides of sliding block DD_iD_{i+1}.

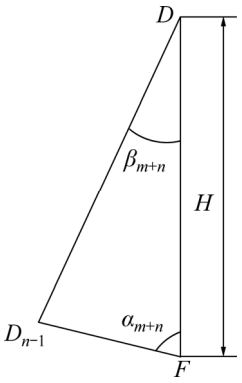

Fig. 7 Geometrical relationship of block $DD_{n-1}F$

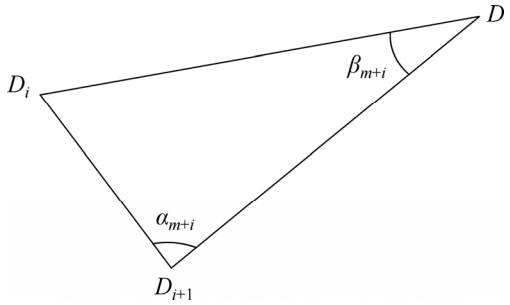

Fig. 8 Geometrical relationship of block DD_iD_{i+1}

From recursive calculation of Eq. (4) and Eq. (5), the length of line $\overline{D_1O_1}$ can be obtained by combining with $\overline{DF}=H$. As shown in Fig. 9, ΔD_1DO_1 is analyzed to get

$$\begin{cases}\theta_1=\arcsin\left[\dfrac{\overline{DO_1}}{\overline{DD_1}}\sin\left(\arctan\dfrac{f}{b}\right)\right]\\ \overline{D_1O_1}=\dfrac{\sin\left(\theta_1+\arctan\dfrac{f}{b}\right)}{\sin\theta_1}\overline{DO_1}\end{cases}\tag{6}$$

where $\overline{D_1O_1}$, $\overline{DO_1}$ and $\overline{DD_1}$ are the lengths of the sides of ΔD_1DO_1, respectively, and $\overline{DO_1}=\sqrt{b^2+f^2}$.

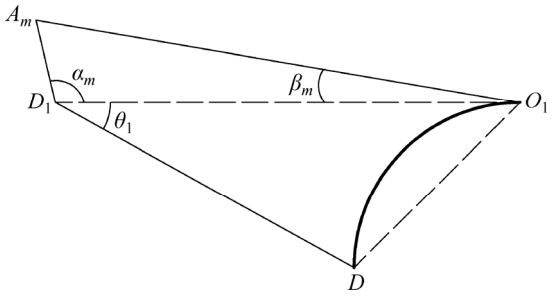

Fig. 9 Geometrical relationship of block $A_mD_1DO_1$

Thus, the same method can be used to get the lengths of the broken lines and fracture lines of the fracture area above the vault (Figs. 9 and 10).

$$\begin{cases}\overline{A_mD_1}=\dfrac{\sin\beta_m}{\sin(\alpha_m+\beta_m)}\overline{D_1O_1}\\ \overline{A_mO_1}=\dfrac{\sin\alpha_m}{\sin(\alpha_m+\beta_m)}\overline{D_1O_1}\end{cases}\tag{7}$$

$$\begin{cases}\overline{A_iA_{i+1}}=\dfrac{\sin\beta_i}{\sin(\alpha_i+\beta_i)}\overline{A_{i+1}O_1}\\ \overline{A_iO_1}=\dfrac{\sin\alpha_i}{\sin(\alpha_i+\beta_i)}\overline{A_{i+1}O_1}\end{cases}\quad(i=1,\cdots,m-1)\tag{8}$$

where $\overline{A_mD_1}$ and $\overline{A_mO_1}$ are the lengths of the sides of the quadrilateral sliding block $A_mD_1DO_1$, respectively, while $\overline{A_iA_{i+1}}$ and $\overline{A_iO_1}$ are the lengths of the sides of triangular sliding block $O_1A_iA_{i+1}$.

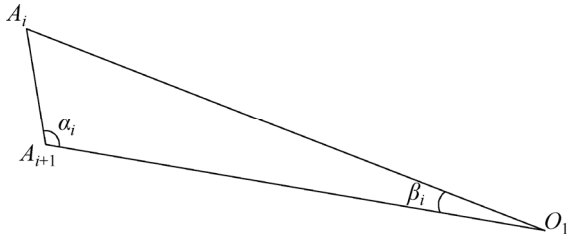

Fig. 10 Geometrical relationship of block $O_1A_iA_{i+1}$

Through the above recursion, the length of $\overline{A_1O_1}$ is obtained, and then the quadrilateral sliding block $AA_1O_1O_2$ is analyzed, as shown in Fig. 11, combined with the associated flow rule:

$$\begin{cases}\overline{AO_2}=\dfrac{(\overline{O_1O_2}-\overline{A_1O_1}\sin\psi)\tan\phi+\overline{A_1O_1}\cos\psi}{\sin\alpha\tan\phi+\cos\alpha}\\ \overline{AA_1}=\dfrac{\overline{AO_2}\cos\alpha-\overline{A_1O_1}\cos\psi}{\sin\phi}\end{cases}\tag{9}$$

where $\overline{AA_1}$, $\overline{AO_2}$ and $\overline{O_1O_2}$ are the lengths of the sides of the sliding block $AA_1O_1O_2$, with $\overline{O_1O_2}=h_1$ and $\psi=\sum_{i=1}^{m}\beta_i$.

For the right side, each velocity vector v_i' and the recursion relation of the length of each dashed line are

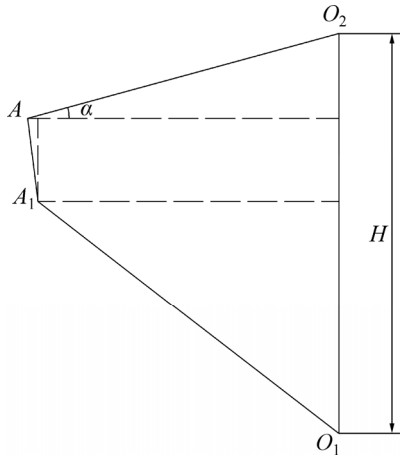

Fig. 11 Geometrical relationship of block $AA_1O_1O_2$

similar to the above derivation, except that $\overline{AA_1}$ is different from $\overline{BB_1}$:

$$\begin{cases} \overline{BO_2}=\dfrac{(\overline{O_1O_2}-\overline{B_1O_1}\sin\psi')\tan\phi+\overline{B_1O_1}\cos\psi'}{\sin\alpha\tan\phi+\cos\alpha} \\ \overline{BB_1}=\dfrac{\overline{BO_2}\cos\alpha-\overline{B_1O_1}\cos\psi'}{\sin\phi} \end{cases} \tag{10}$$

where $\overline{BB_1}$ and $\overline{BO_2}$ are the lengths of the sides of the quadrilateral sliding block $BB_1O_1O_2$; α_i' and β_i' are the included angles between broken line and sliding plane and between adjacent broken lines on the right side of the tunnel, respectively.

4.2 Area of fracture area

Through recursion of the above geometric relations between broken lines or fracture lines, these lengths are obtained, and the area S of each fracture sliding block can be further calculated:

$$\begin{cases} S_{\square\chi\chi_1O_1O_2}=\dfrac{1}{2}\overline{\chi_1O_1}\cos\left(\sum_{i=1}^{m}\zeta_i\right)\left[\overline{\chi_1O_1}\sin\left(\sum_{i=1}^{m}\zeta_i\right)+\overline{\chi\chi_1}\cos\phi\right]+\dfrac{1}{2}\overline{\chi O_2}\left[\overline{\chi O_2}\sin\left(\sum_{i=1}^{m}\zeta_i\right)+\overline{\chi\chi_1}\cos\phi\right] \\ S_{\triangle O_1\chi_i\chi_{i+1}}=\dfrac{1}{2}\overline{\chi_iO_1}\cdot\overline{\chi_{i+1}O_1}\cdot\sin\zeta_i,i=1,\cdots,m-1 \\ S_{\triangle\chi_m\varpi_1O_1}=\dfrac{1}{2}\overline{\chi_mO_1}\cdot\overline{\varpi_1O_1}\sin\zeta_m \\ S_{\triangle\varpi_1\varpi O_1}=\dfrac{1}{2}\overline{\varpi\varpi_1}\cdot\overline{\varpi_1O_1}\sin\xi-\dfrac{\pi bf}{4}+\dfrac{1}{2}bf \\ S_{\triangle\varpi\varpi_i\varpi_{i+1}}=\dfrac{1}{2}\overline{\varpi\varpi_i}\cdot\overline{\varpi\varpi_{i+1}}\cdot\sin\zeta_{m+i},i=1,\cdots,n-2 \\ S_{\triangle\varpi\varpi_{n-1}F(E)}=\dfrac{1}{2}H\cdot\overline{\varpi\varpi_{n-1}}\sin\zeta_{m+n} \end{cases} \tag{11}$$

where χ, ϖ, ζ and ξ are the character variables, and satisfy:

$$\begin{cases} \chi=A,\varpi=D,\zeta=\beta,\xi=\theta_1 \\ \chi=B,\varpi=C,\zeta=\beta',\xi=\theta_1' \end{cases} \tag{12}$$

5 Solution of limit analysis method

5.1 Gravity power

It is assumed that the upper soil reaches the limit state after excavation of the tunnel, and has a trend to slide downwards. The soil belongs to uniform material, and the volume-weight is γ, so the power P_γ generated by the gravity is

$$P_\gamma=P_{\gamma\mathrm{L}}+P_{\gamma\mathrm{R}} \tag{13}$$

where $P_{\gamma\mathrm{L}}$ and $P_{\gamma\mathrm{R}}$ are the gravity power of right and left side of the tunnel, respectively.

where

$$\begin{aligned} P_{\gamma\mathrm{L}}=&\int_S\gamma v_i\mathrm{d}s=\gamma v_0S_{\square AA_1O_1O_2}+\\ &\gamma\sum_{i=1}^{m-1}\left[v_iS_{\triangle O_1A_iA_{i+1}}\sin\left(\alpha_i+\phi-\sum_{j=i+1}^{m}\beta_j\right)\right]+\\ &\gamma v_mS_{\square A_mD_1DO_1}\sin(\alpha_m+\phi)+\\ &\gamma\sum_{i=1}^{n-2}\left[v_{m+i}S_{\triangle DD_iD_{i+1}}\cos\left(\alpha_{m+i}+\phi-\sum_{j=i+1}^{n}\beta_{m+j}\right)\right]+\\ &\gamma v_{m+n-1}S_{\triangle DD_{n-1}\mathrm{F}}\cos(\alpha_{m+n}+\phi) \end{aligned}$$

The calculation formula of $P_{\gamma\mathrm{R}}$ is similar to that of $P_{\gamma\mathrm{L}}$, as long as $A\to B$, $D\to C$, $\alpha\to\alpha'$, $\beta\to\beta'$, $v\to v'$ and $F\to E$.

5.2 Internal energy dissipation power

The internal energy dissipation power P_c of each broken line is given by

$$P_c=P_{c\mathrm{L}}+P_{c\mathrm{R}} \tag{14}$$

where $P_{c\mathrm{L}}$ and $P_{c\mathrm{R}}$ are the internal energy dissipation power of the broken lines on the right and left sides of the tunnel, respectively.

$$\begin{aligned} P_{c\mathrm{L}}=&\int_l(\tau-\sigma\tan\phi)\mathrm{d}l=c\cdot\cos\phi\cdot\left[\overline{AA_1}\cdot v_0+\right.\\ &\sum_{i=1}^{m-1}(\overline{A_iA_{i+1}}\cdot v_i)+\overline{A_mD_1}\cdot v_m+\sum_{i=1}^{n-2}(\overline{D_iD_{i+1}}\cdot v_{m+i})+\\ &\overline{D_{n-1}F}\cdot v_{m+n-1}+\sum_{i=1}^{m}(\overline{A_iO_1}\cdot v_{i-1,i})+\\ &\left.\sum_{i=1}^{n-1}(\overline{D_iD}\cdot v_{m+i-1,m+i})\right] \end{aligned}$$

The calculation formula of $P_{c\mathrm{R}}$ is similar to that of $P_{c\mathrm{L}}$, as long as $A\to B$, $D\to C$, $v\to v'$ and $F\to E$.

5.3 Power of supporting force

Supporting force is the counterforce acting on the

surrounding rocks by supporting structure to prevent the deformation and damage of the surrounding rocks. It is equivalent to surrounding rock pressure, but has an opposite direction, so the power of supporting force is negative. As shown in Fig. 1, it is supposed that the vertical and horizontal loads acting on the supporting structure are q_1, q_2 and e_1, e_2, respectively; they meet assumption 2) in Section 2.1, so the power of supporting force P_T is

$$P_T = \int_l F_i v_i \mathrm{d}l = \frac{b(3q_1+q_2)}{4}\cdot v_m \sin(\alpha_m+\phi) + \frac{b(q_1+3q_2)}{4} v'_m \sin(\alpha'_m+\phi) + k(H+f)\cdot [q_1 v_{m+n}\sin(\alpha_{m+n}+\phi) + q_2 v'_{m+n}\sin(\alpha'_{m+n}+\phi)] \quad (15)$$

where P_T is the power of supporting force.

5.4 Upper-bound solution for surrounding rock pressure

Equations (13) to (15) are substituted into virtual power equation Eq. (16). The load function (q_1, q_2) determined by a set of angles $\{\alpha_i, \beta_i\}$, i=1, ⋯, m+n, rock strength parameter (c, ϕ) as well as tunnel geometric and burial depth parameters (b, f, H, h_1) can be obtained:

$$P_T = P_\gamma - P_c \quad (16)$$

$$(q_1, q_2) = F(\{\alpha_i, \beta_i\}, c, \phi, b, f, H, h_1) \quad (17)$$

Apparently, for any certain project, its rock strength parameter (c, ϕ) as well as tunnel geometric and burial depth parameters (b, f, H, h_1) are already determined in design and investigation stages, so Eq. (17) can be written as

$$(q_1, q_2) = F(\{\alpha_i, \beta_i\}), \quad i = 1, \cdots, m+n \quad (18)$$

From Eq. (18), it can be seen that the load function (q_1, q_2) can be completely determined by a set of angles $\{\alpha_i, \beta_i\}$, i=1, ⋯, m+n.

According to the principle of upper bound method, the maximum load value determined by $\{\alpha_i, \beta_i\}$, i=1, ⋯, m+n is the upper bound solution for surrounding rock pressure of shallow-buried unsymmetrical loading tunnel. However, from Eq. (18), it can be seen that it contains two target parameters q_1 and q_2, and a limiting condition is still required in order to obtain the extreme value of the function. Therefore, it is assumed that

$$q = (q_1 + q_2)/2 \quad (19)$$

Equation (19) is substituted into Eq. (18) to get the function

$$q = F(\{\alpha_i, \beta_i\}), \quad i = 1, \cdots, m+n \quad (20)$$

From the velocity vector diagram shown in Fig. 5, it can be seen that all angle parameters of the left side of the failure mode should meet the corresponding constraint conditions in order to ensure velocity vector closure and geometric boundary condition, so do the right side. Therefore, the upper bound solution for the surrounding rock pressure of shallow-buried unsymmetrical loading tunnel is transformed into the extreme value problem of q determined by Eq. (20):

$$\max q = F(\{\alpha_i, \beta_i\}), \quad i = 1, \cdots, m+n$$
$$\text{s.t.} \begin{cases} \alpha_1 - \sum_{i=2}^{m} \beta_i + \phi - \dfrac{\pi}{2} > 0 \\ \alpha_i - \alpha_{i-1} + \beta_i > 0,\ i = 2, \cdots, m+n \\ \pi - \alpha_{m+n} - \beta_{m+n} - 2\phi > 0 \end{cases} \quad (21)$$

It can be seen that the upper bound solution for the surrounding rock pressure of shallow-buried unsymmetrical loading tunnel can be interpreted as the optimal solution for nonlinear programming of inequations. Through computer programming, the surrounding rock pressure q_1, q_2 and e_1, e_2 can be calculated respectively.

6 Example of verification and analysis

6.1 Example of verification

In order to verify the reliability of the method derived in this work, a typical shallow-buried unsymmetrical loading tunnel is calculated as an engineering case. The result is compared with that by "code method" and test result [1].

The tunnel excavation height is taken as H+f=8 m, span 2b=10 m, specific weight of surrounding rock γ= 19 kN/m^3, cohesion c=30 kPa, internal friction angle ϕ=18°, angle of unsymmetrical loading α=30°, and burial depth h_1=8 m. All calculated results are listed in Table 1. From the analysis on Table 1, it can be seen that:

1) For load q_1 in the shallow side, the relative deviations of the three results are within 10%; for load q_2 in the deep side, the relative deviations between upper bound solutions derived by the proposed method, the code method and test result are relatively large, because the sliding blocks in the example is few, which makes the dissipation of internal energy produced by soil cohesion can not be taken into account totally. Overall, the results calculated by the method proposed are reliable.

2) In addition, the loads are considered as linear distribution, as shown in Fig. 12. It can be seen that the straight slopes obtained by the upper bound method and the model test are obviously larger than the calculated result of code method, which means that the calculated results of current code method underestimate the unsymmetrical loading feature of surrounding rock

Table 1 Comparison of results

Burial depth/m	Bias angle/(°)	Deep-buried side						Shallow-buried side					
		q_2/kPa			Relative difference/%			q_1/kPa			Relative difference/%		
		Code method	Upper bound method	Test value	E_1	E_2	E_3	Code method	Upper bound method	Test value	E_1	E_2	E_3
8	15	162.4	218.3	197.6	34.4	10.5	−17.8	137.2	175.6	132.4	28.0	32.6	3.6
	30	177.2	255.7	209.6	44.3	22.0	−15.5	122.8	125.6	119.6	2.3	5.0	2.7
	45	195.6	283.5	217.6	44.9	30.3	−10.1	102.4	90.4	106.0	−11.7	−14.7	−3.4
28	15	438.8	483.7	508.0	10.2	−4.8	−13.6	418.4	415.6	399.6	−0.7	4.0	4.7
	30	477.2	489.9	582.0	2.7	−15.8	−18.0	430.4	396.3	392.0	−7.9	1.1	9.8
	45	496.0	463.2	630.0	−6.6	−26.5	−21.3	414.8	341.2	387.2	−17.7	−11.9	7.1

Note: E_1=[q(Upper bound method)−q(Code method)]/q(Code method), E_2=[q(Upper bound method)−q(Test value)/q(Test value), and E_3=[q(Code method)−q(Test value)/q(Test value).

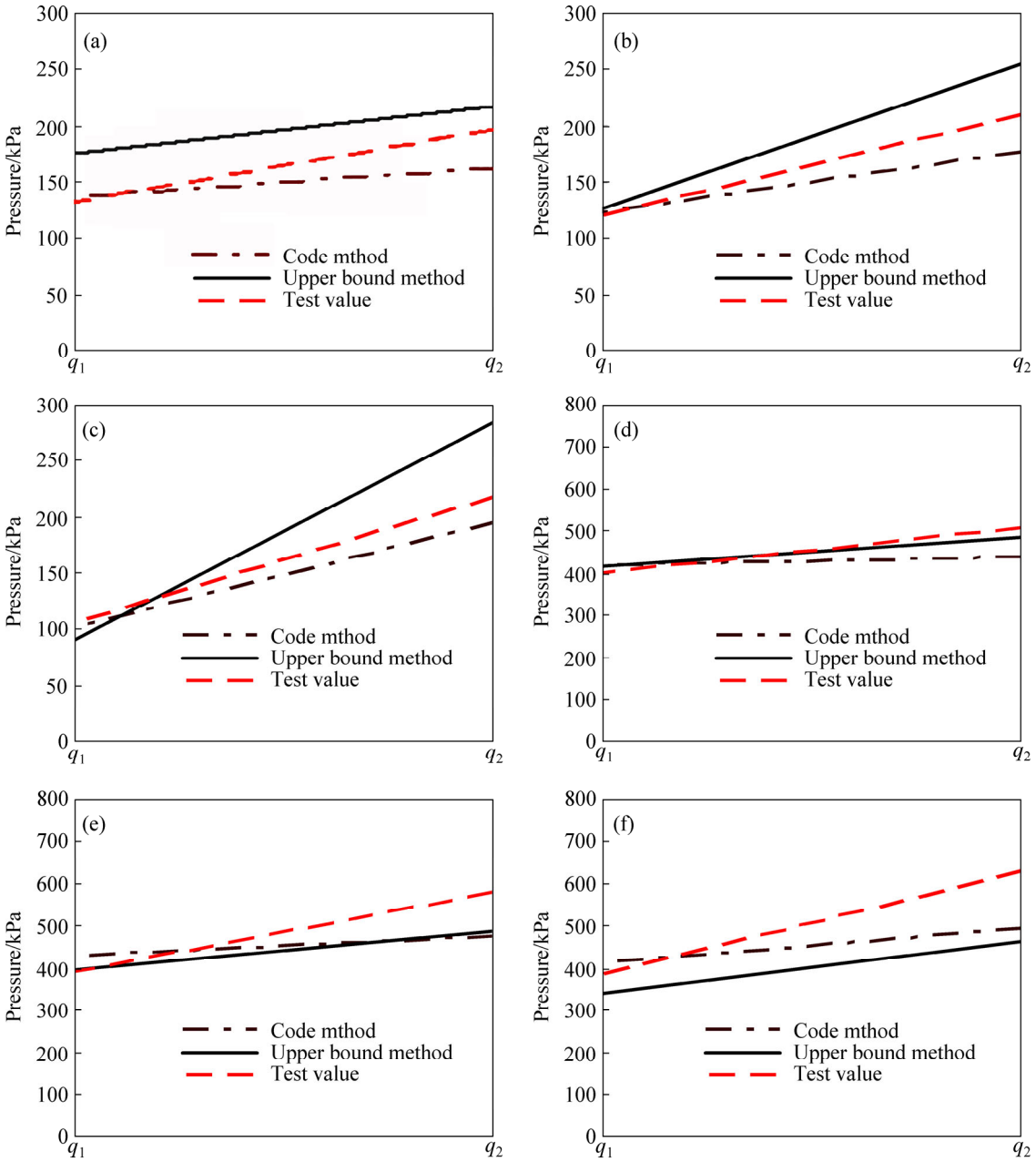

Fig. 12 Comparison of results: (a) h_1=8 m, α=15°; (b) h_1=8 m, α=30°; (c) h_1=8 m, α=45°; (d) h_1=28 m, α=15°; (e) h_1=28 m, α=30°; (f) h_1=28 m, α=45°

pressure. Therefore, the code method is unsafe. These are also consistent with the research conclusions in Ref. [1]. However, the calculated values of code method are obtained based on the assumption that the linear distribution of load is parallel to the unsymmetrical loading line of the terrain. This assumption has some errors and is inconsistent with the actual situation.

6.2 Comparative analysis

In order to further analyze the application of the method derived in this work, the above engineering case is used. The calculation is made under 5 combinations of conditions: burial depth of h_1=28 m and unsymmetrical loading angles of α=15° and 45°. The specific calculated results are shown in Table 1, Figs. 12 and 13.

1) When the burial depth is shallow, the result calculated by the upper bound method is slightly larger than that of code method and model test, but closer to the model test, with the maximum relative deviation of almost 30%; the result calculated by code method has the maximum relative deviation of 45%, and its relative deviation gradually increases with the increase of unsymmetrical loading angle, as reflected by load value of the deep side.

2) When the burial depth is large, the result calculated by the upper bound method lies between that of "code method" and the model test. When the unsymmetrical loading angle is 15°, the three results are extremely close to each other, with the maximum relative deviation of only 10%; when the unsymmetrical loading angle is 45°, the relative deviations of the three results increase, with the maximum value of about 26%.

In general, three results are very close to each other, which further means that the upper bound method is feasible for solving the surrounding rock pressure of shallow-buried unsymmetrical loading tunnels.

3) With the increase of unsymmetrical loading angle, the surrounding rock pressure in deep side gradually increases. The increase amplitude of the upper bound method is larger than that of other two methods; the surrounding rock pressure in shallow side reduces a little, and the three results have similar changes and values. This also verifies the analysis results and conclusions in Ref. [1], i.e. the current code method underestimates the unsymmetrical loading feature of surrounding rock pressure of shallow-buried unsymmetrical loading tunnels.

4) When the test result is taken as the reference value to analyze the relative deviations of the three result in each condition, it can be concluded that when h_1<2D or h_1>2D and α<45°, the result of the proposed method or the average values taken of both the proposed method and code method are more reasonable, and can more accurately reflect the unsymmetrical loading feature. When h_1>2D and α≥45°, the code method is more suitable.

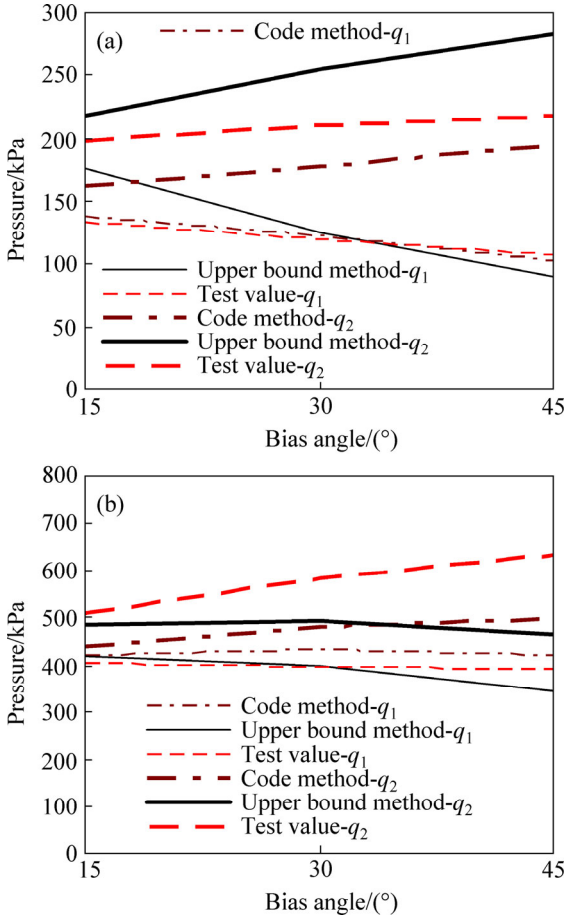

Fig. 13 Change laws of surrounding rock pressure on bias angles: (a) h_1=8 m; (b) h_1=28 m

7 Conclusions

1) Combined with the analysis results of laboratory model test, the failure mode of shallow-buried unsymmetrical loading tunnels is established. The corresponding velocity field is built based on the associated flow rule, and the upper bound solution for the surrounding rock pressure is derived based on the principle of virtual power.

2) Example analysis results show that the upper bound method is feasible for solving the surrounding rock pressure of shallow-buried tunnels under unsymmetrical loading, while the current code method underestimates the unsymmetrical loading feature, and it is unsafe.

3) Through discussion on the application of the current code method and the proposed method, it can be concluded that when h_1<2D or h_1>2D and α<45°, the result by the proposed method or the average values taken of both the proposed method and code method are more reasonable, and more accurately reflect the

unsymmetrical loading feature. When $h_1>2D$ and $\alpha\geq45°$, the code method is more suitable.

References

[1] LEI Ming-feng, PENG Li-min, SHI Cheng-hua, WANG Li-chuan, LIU Zheng-chu. Model research on failure mechanism and lining stress characteristics of shallow buried tunnel under unsymmetrical pressure [J]. Journal of Central South University (Science and Technology), 2013, 44(8): 3316−3325. (in Chinese)

[2] LEI Ming-feng, PENG Li-min, SHI Cheng-hua. Calculation of the surrounding rock pressure on a shallow buried tunnel using linear and nonlinear failure criteria [J]. Automat Constr, 2014, 37: 191−195.

[3] DAVIS E H, DUNN M J, MAIR R J, SENEVIRATNE H N. The stability of shallow tunnels and underground openings in cohesive material [J]. Geotechnique, 1980, 30(4): 397−416.

[4] JTG D70—2004, Code for design of road tunnel [S]. Beijing: China Communications Press, 2004. (in Chinese)

[5] TB 10003—2005, J449-2005. Code for design on tunnel of railway [S]. Beijing: China Railway Press, 2001. (in Chinese)

[6] ATKINSON J H, POTTS D M. Stability of a shallow circular tunnel in cohesionless soil [J]. Geotechnique, 1977, 27(2): 203−215.

[7] HUANG Fu, ZHANG Dao-bing, SUN Zhi-bin, JIN Qi-yun. Upper bound solutions of stability factor of shallow tunnels in saturated soil based on strength reduction technique [J]. Journal of Central South University, 2012, 19(7): 2008−2015.

[8] LECA E, DORMIEUX L. Upper and lower bound solutions for the face stability of shallow circular tunnels in frictional material [J]. Geotechnique, 1990, 40(4): 581−606.

[9] JIANG Gong-liang. Limit analysis of the stability of shallow tunnels in soft ground [J]. China Civil Engineering Journal, 1998, 31(5): 65−72. (in Chinese)

[10] YANG Xiao-li, HUANG Fu. Collapse mechanism of shallow tunnel based on nonlinear Hoek-Brown failure criterion [J]. Tunnel Under Space Tech, 2011, 26(6): 686−691.

[11] YANG Xiao-li, WANG Jin-ming. Ground movement prediction for tunnels using simplified procedure [J]. Tunnel Under Space Tech, 2011, 26(3): 462−471.

[12] YANG Xiao-li, ZHANG Jia-hua, JIN Qi-yun, MA Jun-qiu. Analytical solution to rock pressure acting on three shallow tunnels subjected to unsymmetrical loads [J]. Journal of Central South University, 2013, 20: 528−535.

[13] YANG Xiao-li, ZHANG Dao-bing, WANG Zuo-wei. Upper bound solutions for supporting pressures of shallow tunnels with nonlinear failure criterion [J]. Journal of Central South University, 2013, 20: 2034−2040.

[14] YANG Feng, YANG Jun-sheng. Limit analysis method for determination of earth pressure on shallow tunnel [J]. Engineering Mechanics, 2008, 25(7): 179−184. (in Chinese)

[15] FRALDI M, GUARRACINO F. Analytical solutions for collapse mechanisms in tunnels with arbitrary cross sections [J]. Int J Solids Struct, 2010, 47(2): 216−223.

(Edited by FANG Jing-hua)